Received: 13 March 2018 | Revised: 26 May 2018 | Accepted: 13 June 2018
DOI: 10.1002/aoc.4504

FULL PAPER

WILEY Applied Organometallic Chemistry

Supramolecular assembly of hydrogen bonding, ESR studies and theoretical calculations of Cu(II) complexes

Sh.M. Morgan[1] | M.A. Diab[2] | A.Z. El-Sonbati[2]

[1] Environmental Monitoring Laboratory, Ministry of Health, Port Said, Egypt
[2] Chemistry Department, Faculty of Science, Damietta University, Damietta, Egypt

Correspondence
M. A. Diab, Chemistry Department, Faculty of Science, Damietta University, Damietta, Egypt.
Email: m.adiab@yahoo.com

A series of copper(II) complexes were synthesized by the reaction of copper(II) chlorid with 1-phenyl-3methyl-(3-dervitives phenylhydrazo)-5-pyrazolone (HL_n) yields 1:1 and 1:2 (M:L) complexes depending on the reaction conditions. The elemental analysis, spectral (IR, ^{1}H NMR, UV-Vis and ESR), conductance and magnetic measurements were used to characterize the isolated complexes. The IR spectral data indicate that the metal ions are coordinated through the oxygen of the keto and nitrogen of hydrazone groups. The UV-Vis spectra, magnetic moments and ESR studies indicate square planar geometry for Cu(II) complexes (**1–3**) by NO monobasic bidentate and the two monobasic *trans* bidentate in octahedral geometry for Cu(II) complexes (**4–6**). It is found that the change of substituent affects the theoretical calculations of Cu(II) complexes. Molecular docking was used to predict the binding between the ligands (HL_n) and the receptors of prostate cancer mutant (2Q7K), breast cancer mutant (3HB5), crystal structure of *E. coli* (3T88) and crystal structure of *S. aureus* (3Q8U). The molecular and electronic structures of Cu(II) complexes and quantum chemical calculations were studied. According to intramolecular hydrogen bond leads to increasing of the complexes stability.

KEYWORDS
Cu(II) supramolecular structure, ESR study, molecular docking, molecular structures, pyrazolone derivatives

1 | INTRODUCTION

Aromatic azo dyes are the most widely used class of coloring materials due to their massive application in various fields of science and technology.[1–3] The photo-physical and photo-chemical properties of this class of dyes make them suitable as optical sensors and advanced materials. Furthermore, azo compounds are known to be involved in a number of biological reactions such as inhibition of DNA, and biological activity against bacteria and fungi.[4–9] The azo/hydrazone tautomerism in azo compounds is very attractive from theoretical and practical viewpoints and has been of particular interest.[4–6] It is described by the intramolecular proton transfer between the phenol and imine groups in ground and/or excited state.[10] The presence of azo/hydrazone tautomerism in these compounds may influence considerably in their unique photo-physical and photo-chemical properties, which is turn strongly influenced by several factors including temperature, the substituent structure and solvent polarity.[11]

Cu(II) complexes have received much attention because of their rich electrochemical and photophysical properties as well as their potential applications in various supramolecular structures.[12–14] Multinuclear systems of this kind can be developed by covalent linking of building blocks with spacers which, therefore, is the key component because the size, shape and electronic nature of the bridge controls the electronic communication between the chromophores and thereby the molecule as a whole.

The present study describes the chelation behavior of Cu(II) complexes **(1–6)** of 1-phenyl-3-methyl-(3-derivatives phenylazo)-5-pyrazolone (HL_n) (where *n* = 1; COOH (HL_1), *n* = 2; OH (HL_2) and *n* = 3; OCH_3 (HL_3)). R = COOH (HL_1); R = OH (HL_2) and R = OCH_3 (HL_3). The structure of the Cu(II) complexes **(1–6)** is elucidated using elemental analysis, IR, electron spin resonance (ESR), UV–Vis spectra, magnetic moment and molar conductance. Molecular docking was used to predict the binding between HL_n and the receptors of prostate cancer mutant (2Q7K), breast cancer mutant (3HB5), crystal structure of *E. coli* (3T88) and crystal structure of *S. aureus* (3Q8U). Theoretical study of Cu(II) complexes **(1–6)** were optimized theoretically and the quantum chemical parameters were calculated.

2 | EXPERIMENTAL

2.1 | Material and reagents

The standard chemicals, 3-methyl-1-phenyl-1H-pyrazol-5(4H)-one and 3-alkyl anilines (alkyl: OCH_3, COOH and OH; Aldrich Chemical Co.), sodium nitrite, hydrochloric acid and ethanol were used without any further purification.

2.2 | Preparation of 1-phenyl-3-methyl-(3-derivatives phenylazo)-5-pyrazolone (HL_n)

In a typical preparation, 25 ml of distilled water containing 0.01 mol hydrochloric acid were added to *m*-derivatives aniline (0.01 mol).[15] To the resulting mixture stirred and cooled to 0 °C, a solution of 0.01 mole sodium nitrite in 20 ml of water was added dropwise. The formed diazonium chloride was consecutively coupled with an alkaline solution of 0.01 mol 3-methyl-1-phenyl-1H-pyrazol-5(4H)-one as shown in Figure 1. The colored precipitate, which formed immediately, was filtered through sintered glass crucible, washed several times with water. Table S1 shows the details of elemental analysis of the ligands.

2.3 | Preparation of complexes

For the synthesis of copper complexes; a solution of $CuCl_2.2H_2O$ in approximately 50 ml of absolute alcohol was mixed with an appropriate amount of HL_n ligands to give a molar ratio of 1:1/1:2(M:L_n). Reflux was

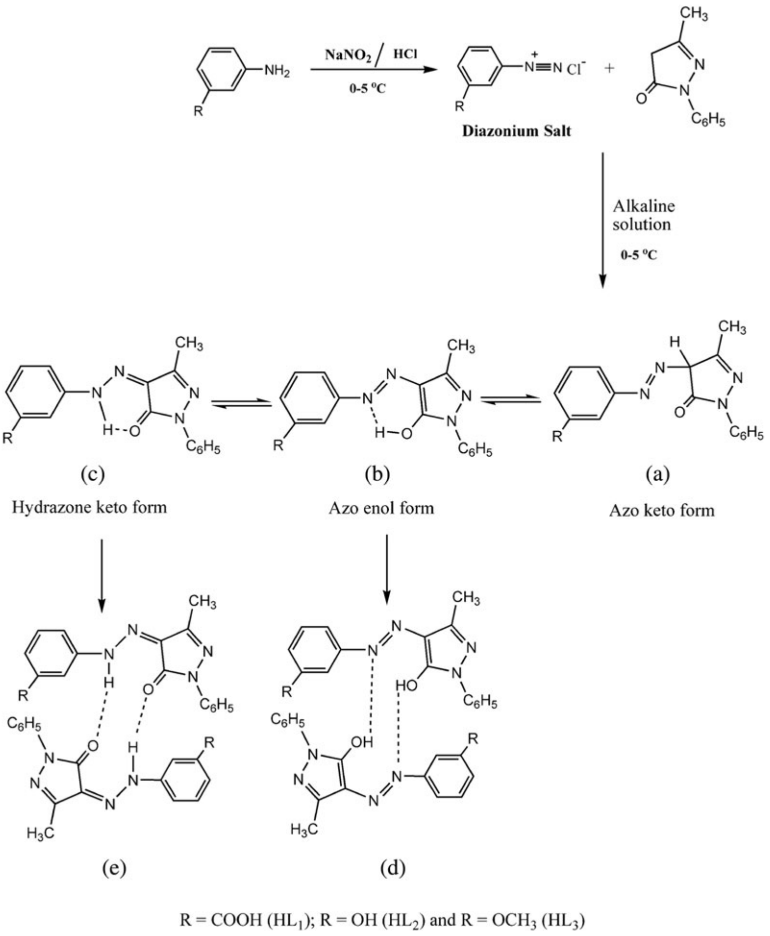

FIGURE 1 The formation mechanism and tautomeric forms of ligands (HL_n)

continued for ~ 2 hrs, followed by removal of the excess solvent under reduced pressure. The complexes were filtered and washed with Et_2O.

All precipitates were dried in a vacuum oven at 40 °C for several days. Table 1 shows the details of elemental analysis of the isolated complexes.

2.4 | Measurements

Elemental microanalyses of the separated ligands and solid chelates for C, H and N were performed in the Microanalytical Center, Cairo University, Egypt. The analyses were repeated twice to check the accuracy of the analyzed data. The metal content in the complexes was estimated by standard methods.[16] The ^1H NMR spectrum was obtained with a JEOL FX90 Fourier transform spectrometer with DMSO-d_6 as the solvent and TMS as an internal reference. The infrared spectra were recorded as KBr discs using a Perkin-Elmer 1340 spectrophotometer. Ultraviolet–Visible (UV–Vis) spectra of the compounds were recorded in Nuzol solution using a Unicom SP 8800 spectrophotometer. The magnetic moment of the prepared solid complexes was determined at room temperature using the Gouy's method. Mercury(II) (tetrathiocyanato cobalt(II)), $[Hg\{Co(SCN)_4\}]$, was used for the calibration of the Gouy's tubes. Magnetic moments were calculated using the equation, $\mu_{eff.} = 2.84\ [T\ \chi_M^{coor.}]^{1/2}$. Electron spin resonance (ESR) measurements of powdered samples were recorded at room temperature using an X-band spectrometer utilizing a 100 kHz magnetic field modulation with 2,2-diphenyl-1-picrylhydrazyl (DPPH) as a reference material.

Docking process in which the ligand–protein interaction energies are calculated using a Docking Server.[17,18] Docking calculations were carried out on prostate cancer mutant (2Q7K), breast cancer mutant (3HB5), crystal structure of *E. coli* (3T88) and crystal structure of *S. aureus* (3Q8U) protein models. Essential hydrogen atoms, Kollman united atom type charges, and solvation parameters were added with the aid of AutoDock tools.[19,20] Auto Dock parameter set- and distance-dependent dielectric functions were used in the calculation of the van der Waals and the electrostatic terms, respectively.

The molecular structures of the compounds were optimized by HF method with 3-21G basis set. The molecules were built with the Perkin Elmer ChemBio Draw and optimized using Perkin Elmer ChemBio3D software.[21–24] Quantum chemical parameters such as the highest occupied molecular orbital energy (E_{HOMO}), the lowest unoccupied molecular orbital energy (E_{LUMO}) and HOMO–LUMO energy gap (ΔE) for the investigated molecules were calculated.

3 | RESULTS AND DISCUSSION

3.1 | The solid state structures

In general, most of the azo compounds give spectral localized bands in the wavelength range 46620–34480 and 31250–270370 cm^{-1}. The first region is due to the absorption of the aromatic ring compared to ^1B_b and ^1L_b of mono substituted benzene while the second region is due to the conjugation between the azo group and the aromatic nuclei, with intermolecular charge transfer resulting from π-electron migration to the diazo group from electron donating substituents. The position of the π-π* transition of the azo groups remains is one of the most interesting unresolved questions of molecular spectroscopy.[25]

The principal ligands (HL_n) were synthesized by coupling of 3-methyl-1-phenyl-1H-pyrazol-5(4H)-one with diazonium salts. The elemental analysis is in good agreements with the proposed structure, 1-phenyl-3-methyl-(3-derivatives phenylazo)-5-pyrazolone (HL_n) can exist either as the keto or enol form or as an equilibrium mixture of the two since it has a hydrazone function. However, the IR and NMR spectra of HL_n indicate that in

TABLE 1 Elemental analysis data for Cu(II) complexes

		Exp. (calcd.)%			
Compound	$\mu_{eff.}$ **(B.M.)**	**C**	**H**	**N**	**M**
$[CuL_1(Cl)(OH_2)]$(1)	1.89	46.47 (46.57)	3.29 (3.42)	12.58 (12.78)	14.31 (14.51)
$[CuL_2(Cl)(OH_2)]$(2)	1.90	46.57 (46.82)	3.52 (3.66)	13.38 (13.66)	15.35 (15.50)
$[CuL_3(Cl)(OH_2)]$(3)	1.91	48.05 (48.11)	3.95 (4.01)	12.88 (13.21)	14.56 (14.99)
$[Cu(L_1)_2(OH_2)_2]$(4)	2.05	55.07 (55.02)	3.92 (4.05)	14.78 (15.10)	8.31 (8.57)
$[Cu(L_2)_2(OH_2)_2]$(5)	1.93	56.07 (56.01)	4.28 (4.38)	16.18 (16.34)	9.01 (9.27)
$[Cu(L_3)_2(OH_2)_2]$(6)	2.15	56.97 (57.18)	4.57 (4.77)	15.58 (15.70)	8.51 (8.91)

solid state it remains in the keto form. This indicates that in solution and presence of metal, it converts to enol/ hydrazone form and coordinates to the metal in the hydrazone-keto form.[26]

The elemental analysis corresponds to the general formulae [Cu $(L_n)(Cl)(OH_2)$] **(1–3)** and [Cu $(L_n)_2(OH_2)_2$] **(4–6)** for all complexes. The principal ligands (HL_n) undergoes mono deprotonation to form L_n in copper complexes and act as a bidentate ligand thus occupying one/two positions of a square planar/octahedral geometry. The chloride and aqua/two aqua groups occupy the four/sixth position. All complexes exhibited non-conducting properties in DMF solution.

3.2 | Stoichiometries of the copper(II) complexes

The stoichiometries of the complexes have been deduced from their elemental analyses. HL_n is mononucleating and hence requires one metal ion for coordination. All the products were partially soluble in common organic solvents. On the basis of elemental analysis (Table 1), the compositions of the complexes agree well with their structural formulae.

Copper chloride reacts with the HL_n in 1:1/1:2 (metal: ligand) mole ratios in anhydrous alcohol, giving partially soluble products as indicated below.

The formation of the complexes may be represented by the following reactions.

1 Complexes with half equivalent anions.
The ligands behave as a monobasic and one contain one anion (chloride ion).

$$HL_n + CuCl_2.2H_2O \quad \rightarrow [CuL_n(Cl)(OH_2)]$$

2 Complexes deprived of the anions.
In this case the anions of the copper salt are eliminated in the reaction medium as the corresponding acid on the following the Cu^{2+} salt to react with the ligands.

$$2HL_n + CuCl_2.2H_2O \quad \rightarrow \left[Cu\ (L_n)_2(OH_2)_2\right]$$

3.3 | Molar conductance of the copper(II) complexes

The conductance measurements, of solutions of copper(II) complexes (10^{-3} M in DMSO) show the value in the range of 7–11 Ω^{-1} cm^2 mol^{-1}. These values suggest that all copper(II) complexes are non-electrolyte in nature.[12]

3.4 | Infrared spectra and nature of coordination

The bonding of the metal ion to the ligands can be clarified by comparing the IR spectra of the complexes with those of the ligands. Microanalytical data as well as metal, and cholride estimations are in good agreement with stoichiometry proposed for complexes (Figure 2 and Table 1). The following conclusions can be drowning:

1 The infrared spectra of ligands exhibit a strong band at 1645–1625 cm^{-1} due to υ (C=O) (pyrazolone ring).[27] The discussed infrared features beside the band appeared at ~1595–1575 cm^{-1}, can guide to assume the presence of υ (C=N-) (hydrazone group) structure through resonating phenomena.[9] In general, the presence of electron attracting group minimizes the charge transfer from the phenyl ring and this leads to increase the C=O band modes. The βC-H, δC-H and γC-H modes of vibrations are identified by the presence of strong bands in the 1180–1110, 1030–930 and 840–780 cm^{-1} region, respectively. The C–C vibrations also are identified by the presence of several bands at frequencies lower than 755 cm^{-1}. Generally, the electron donor methoxy group enhances the change transfer from the phenyl ring to the heterocyclic moiety.[28,29] This leads to increase both polarizability of the carbonyl group. Such class of compounds as illustrated in (Figure 1) has different types of hydrogen bonding according to El-Sonbati *et al.*,[30,31] as follows:
   i. H-bonding of the type O–H····N between the –OH group and –N=N– group (Figure 1. (B)).
   ii. H-bonding of the type N–H····O between the –NH group and C=O group (Figure 1. (C)).

2 Intermolecular hydrogen bonding of the O–H····N (Figure 1. (D)) or N–H····O (Figure 1. (E)) shows type of one molecule to another as given in Figure 1.
3 The case (2) is more favored than case (1). This is due to the presence of broad band located at 875–975 cm^{-1},

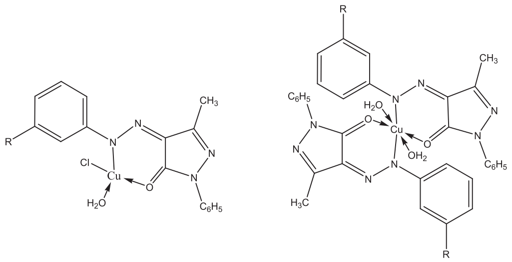

(1-3)

(4-6)

R = COOH; R = OH and R = OCH_3

FIGURE 2 The structures of Cu(II) complexes which could be taken as a good evidence for the intramolecular hydrogen bonding.[5,9]

In the ^{1}H NMR spectrum of the HL_3 measured in DMSO-d_6 (Table S2), the hydrogen proton appear as a singlet at 11.32 ppm, which corresponds to NH proton resonance of the hydrazone form.[5] The above results suggest that the ligand exists in the keto hydrazone form.

By comparing the infrared spectra of free ligands to that of the prepared complexes the following points are observed.

1. The infrared spectra of the free ligands show no characteristic absorption assignable to NH_2 function. This confirms the formation of the azo compounds.
2. In all complexes bands at 3480–3150 cm^{-1} are observed. Such region is attributed to different probabilities: (a) it is due to either free OH or NH; (b) bonded –OH group or –NH group; or (c) due to presence of water molecules.
3. The absence of any peak attributed to the -N=N- moiety, implies that the ligands exist predominantly in solution as the form shown in Figure 1. However, in solution and in the presence of Cu(II) ion these compounds exist in a tautomeric equilibrium 1B↔1C. The main change is observed in the azo stretching vibration, thus suggesting that the form shown in Figure 1. Prevails this tautomeric form losses hydrazone proton when complexed with Cu(II) ion as mononegative chelating agents produces the C=N-NH mode of the free ligands. New bands assigned to υ (NH) in the free ligands is absent, suggesting the cleavage of intramolecular hydrogen bonding of υNH group and coordination of nitrogen to the metal ion.

According to the structure shown in Figure 1, the HL_n ligands take its usual anionic (L_n) to chelate Cu(II) through N-of hydrazone group and oxygen atom of carbonyl group (Figures 1 and 2) as the potential binding sites, whereas the chloride/aqua anion just fit the remaining free coordination position.

- The sharp, medium intensity band of (C=N-) (hydrazone) appears at 1595–1575 cm^{-1} for ligands.
- The strong band observed at 1124–1140 cm^{-1}, which may be assigned to υ (N-N) vibration modes[5,9] is affected on complexation. It is blue shifted and appeared as a weak band.
- The spectra exhibits a strong band at ~ 1650 cm^{-1}, which is indicative to υ (C=O). However, the broad band located at 3430 cm^{-1} leads to characterize the υNH rather than hydrogen bonded –OH with N=N. This is rather confirmed from the observation of Karabatoses et al.[32] where the hydrazone formed is more than the azo structure for similar compounds.
- The carbonyl absorption band υ (CO) (of the pyrazolone ring) was shifted to frequencies higher by 25–10 cm^{-1} for all complexes. The change in the carbonyl band position in the IR spectra of the metal complexes indicates that the carbonyl group in the hydrazone pyrazolone compounds is coordinated to the metal ions (Figure 2).
- The disappearance of the υ (NH) stretching frequency for ligands on chelate formation may be caused by coordination of the hydrazo-nitrogen to the metal ion upon complexation (Figure 1).
- Introduction of a hydrazone group instead of N=N leads to a change in the coordination mode of the azo group from the azo-nitrogen to the amine nitrogen (NH) (Figure 1).
- Coordination of the carbonyl oxygen and the nitrogen of hydrazone in the chelate ring is supported by the appearance of new bands which are assigned to υ (Cu–N) and υ (Cu–O).
- The ligand orbitals of hydrazone pyrazolones are group theoretically, energetically and occupationally suitable for participation in both donor (Cu → L) and acceptor (L → Cu) π-interactions with the copper ion.[12] Convincing evidence has been adduced that Cu → L π-bonding makes a significant contribution to the bonding in copper complexes.
- The spectra of copper(II) complexes reveal the presence of band at ~ 3460 cm^{-1} due to the vibrational frequency of O-H of coordinated water. The presence of coordinated water is further confirmed by the rocking band at ~ 840 cm^{-1} and twisting band at ~ 730 cm^{-1}.

3.5 | Molecular geometry optimization of Cu(II) complexes

The optimized structures of Cu(II) complexes are given in Figure 3. The selected geometrical structures of Cu(II) complexes were calculated by optimizing their bond lengths and bond angles (Tables S3-S8). Quantum chemical parameters such as the highest occupied molecular orbital energy (E_{HOMO}), the lowest unoccupied molecular orbital energy (E_{LUMO}) and HOMO–LUMO energy gap (ΔE) for the investigated molecules were calculated.

In Figure 4 the HOMO–LUMO energy gap, ΔE, which is an important stability index, is applied to develop theoretical models for explaining the structure and conformation barriers in many molecular systems.[27] The complexes **(1)** and **(4)** are more reactive than other complexes as reflected from energy gap values. The calculated quantum chemical parameters

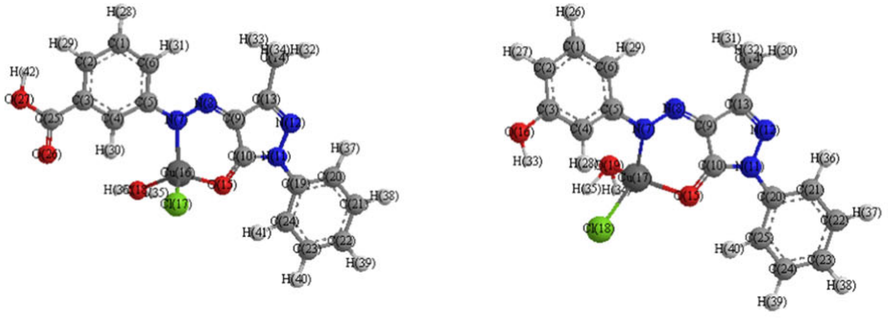

Complex (1)

Complex (2)

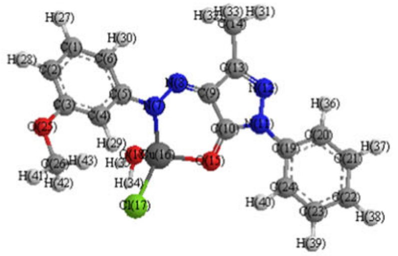

Complex (3)

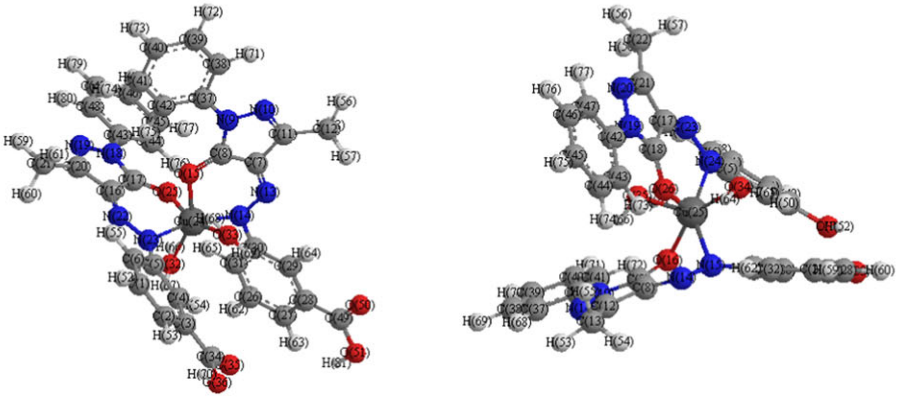

Complex (4)

Complex (5)

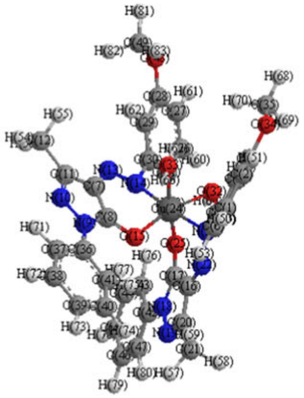

Complex (6)

FIGURE 3 Optimized structures of Cu(II) complexes

are given in Table 2. Additional parameters such as ΔE, absolute electronegativities, χ, chemical potentials, Pi, absolute hardness, η, absolute softness, σ, global softness, S, and additional electronic charge, ΔN_{max}, have been calculated according to the following equations:[21]

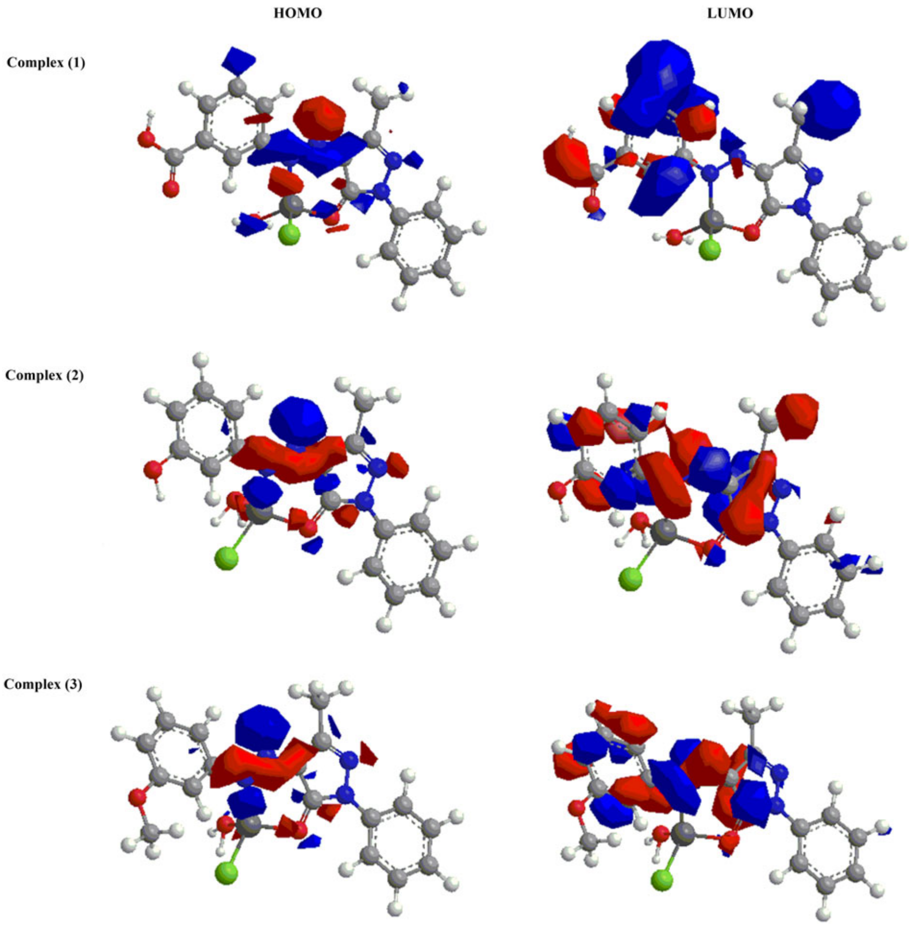

FIGURE 4 The highest occupied molecular orbital (HOMO) and the lowest unoccupied molecular orbital (LUMO) of Cu(II) complexes **(1–6)**

$$\Delta E = E_{LUMO} - E_{HOMO}$$

$$\chi = \frac{-(E_{\mathrm{HOMO}} + E_{\mathrm{LUMO}})}{2}$$

$$\eta = \frac{E_{\mathrm{LUMO}} - E_{\mathrm{HOMO}}}{2}$$

$$\sigma = \frac{1}{\eta},$$

$$Pi = -\chi$$

$$S = \frac{1}{2\eta},$$

$$\Delta N_{\max} = -\frac{Pi}{\eta}$$

3.6 | Molecular docking

The molecular docking is a key tool in computer drug design.[5,9] Molecular docking aims to achieve an optimized conformation for both the protein and drug with relative orientation between them such that the free energy of the overall system is minimized.[17]

In this context, we used molecular docking between ligands (HL_n) and receptors of prostate cancer mutant (2Q7K), breast cancer mutant (3HB5), crystal structure of *E. coli* (3T88) and crystal structure of *S. aureus* (3Q8U). The results showed a possible arrangement between the ligands (HL_n) and the receptors (2Q7K, 3HB5, 3T88 and 3Q8U). The docking study showed a favorable interaction between the ligands (HL_n) and the receptors (2Q7K, 3HB5, 3T88 and 3Q8U) as shown in Figures 5–8 and the calculated energy is listed in Table 3. According to the results obtained in this study, HB plot curve indicates that the ligands (HL_n)) binds to the proteins with hydrogen bond interactions and decomposed interaction energies in kcal/mol were exist between ligands (HL_n) with receptors of prostate cancer mutant (2Q7K), breast cancer mutant (3HB5), crystal structure of *E. coli* (3T88) and crystal structure of *S. aureus* (3Q8U) as shown in Figures S1-S4. 2D plot curves of docking with ligands (HL_n) are shown in Figures S5-S8. The ligand (HL_1) shows best interaction with the receptors (3HB5, 3T88 and 3Q8U) than other ligands (HL_2 and HL_3). Also, the ligand (HL_1) shows best interaction with receptor of breast cancer mutant (3HB5) than other receptors.

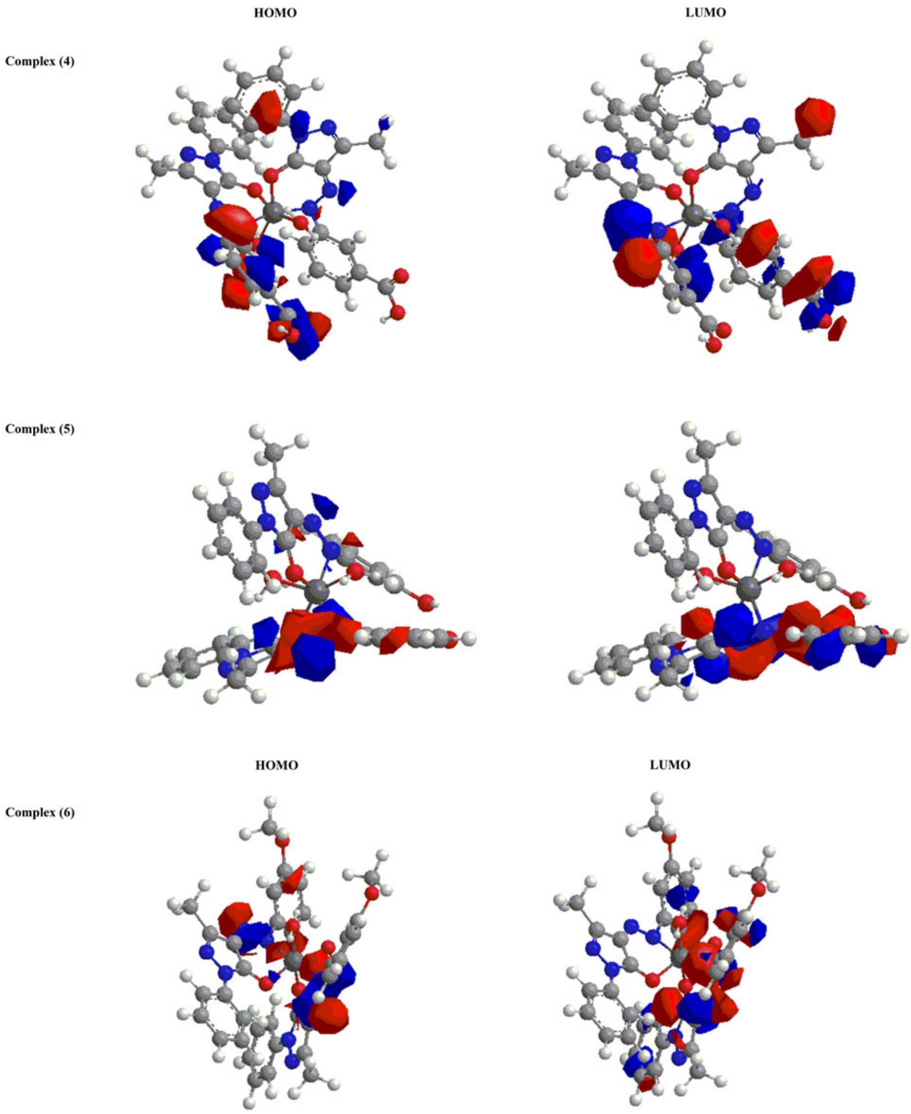

FIGURE 4 Continued.

TABLE 2 The calculated quantum chemical parameters of Cu(II) complexes

Complex[a]	E_{HOMO} (eV)	E_{LUMO} (eV)	ΔE (eV)	χ (eV)	η (eV)	σ $(eV)^{-1}$	Pi (eV)	S $(eV)^{-1}$	ω (eV)	ΔN_{max}
(1)	−4.167	−3.909	0.258	4.038	0.129	7.752	−4.038	3.876	2.019	31.302
(2)	−4.491	−2.184	2.307	3.338	1.154	0.867	−3.338	0.433	1.669	2.893
(3)	−4.509	−2.159	2.350	3.334	1.175	0.851	−3.334	0.426	1.667	2.838
(4)	−2.975	−2.717	0.258	2.846	0.129	7.752	−2.846	3.876	1.423	22.062
(5)	−6.240	−2.569	3.671	4.405	1.836	0.545	−4.405	0.272	2.202	2.399
(6)	−2.177	−1.079	1.098	1.628	0.549	1.822	−1.628	0.911	0.814	2.965

[a] Numbers as given in Table 1.

3.7 | Magnetic moment and electronic spectra studies

The room temperature magnetic moment values for the complexes are characteristic magnetically diluted copper(II) complexes as shown in Table 1, are characteristic of magnetically diluted copper(II) complexes. The higher magnetic moment values than the spin only (1.73 B.M.) imply the presence of a low lying excited term which is able to mix some of its orbital angular

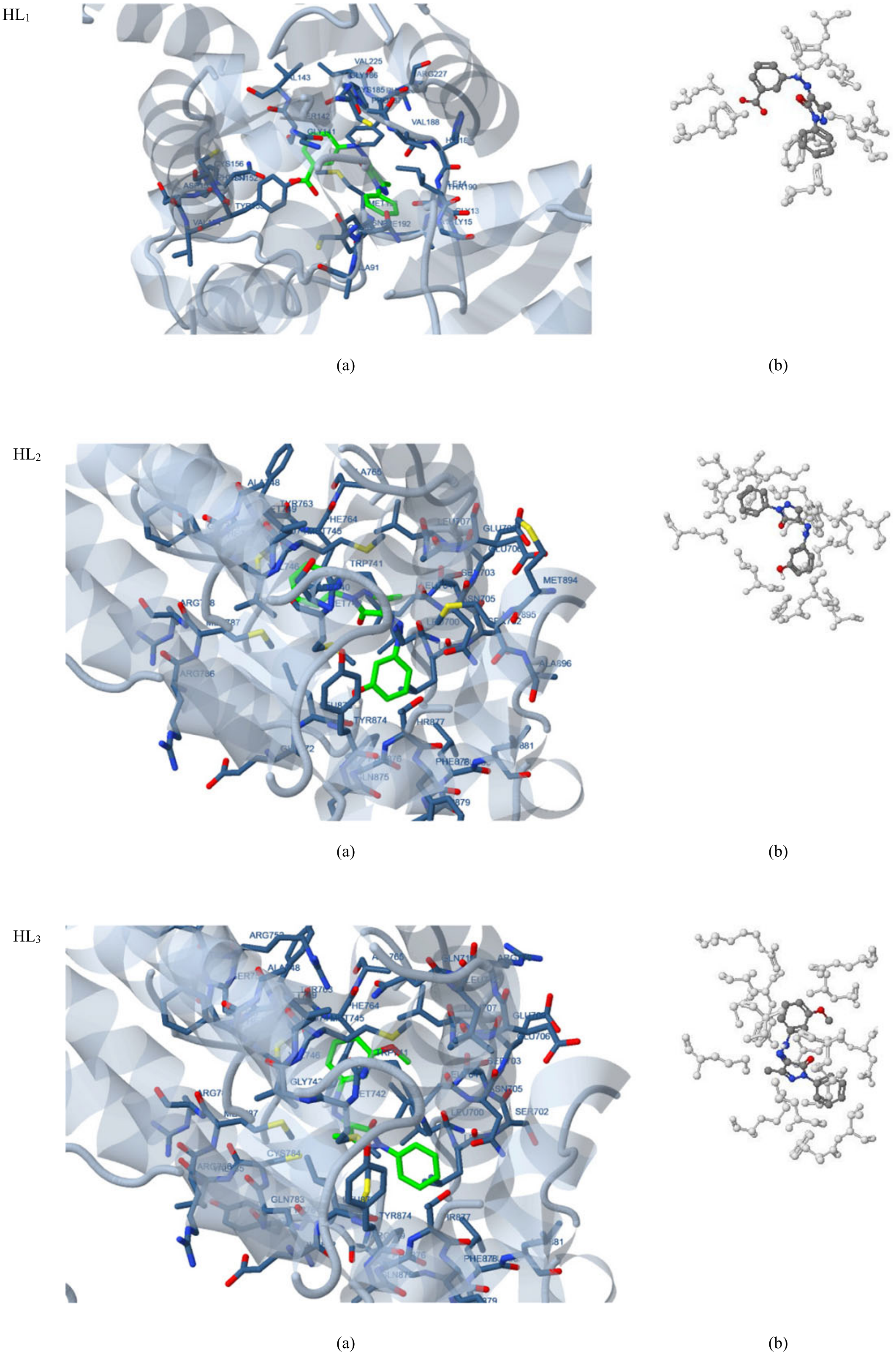

FIGURE 5 Ligands (HL$_n$) (green in (a) and gray in (b)) in interaction with receptor of prostate cancer mutant (2Q7K). (For interpretation of the references to color in this figure legend, the reader is referred to the web version of this article)

momentum with the spin angular momentum of the ground state.[33]

The electronic spectra of the free ligands display bands at ~ 45400–45700, 42120–43320 and 31100–32340 cm^{-1}

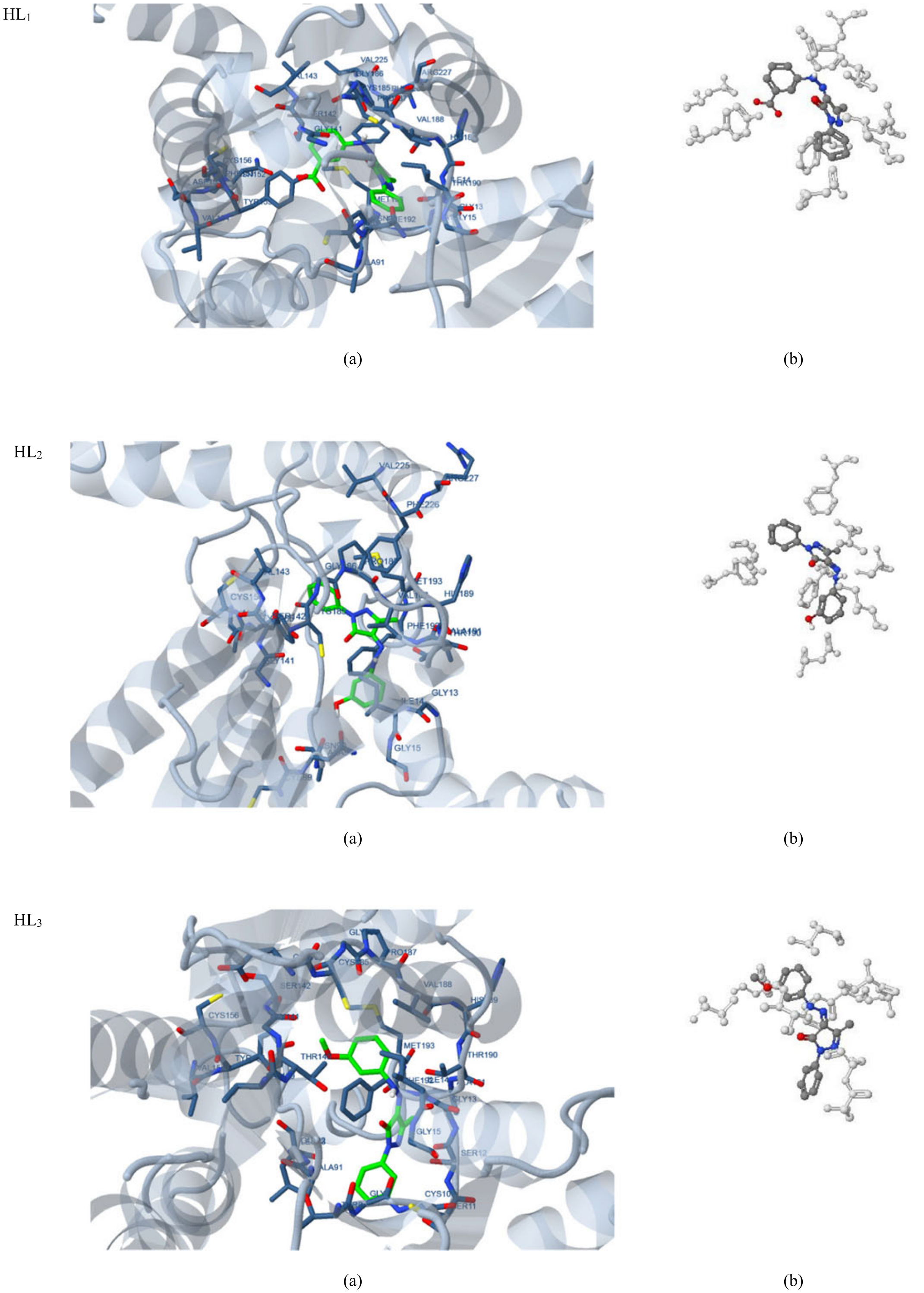

FIGURE 6 Ligands (HL$_n$) (green in (a) and gray in (b)) in interaction with receptor of breast cancer mutant (3HB5). (For interpretation of the references to color in this figure legend, the reader is referred to the web version of this article)

regions are assigned to Ph-Ph*, π-π* (phenyl) and n-π*, respectively. In all complexes, the first band is replaced by a new intense one at 36000–36800 cm^{-1} assignable to $\sigma_{(N)} \rightarrow Cu^{2+}$ charge transfer transition. The new band appeared at 25350–26300 cm^{-1} in the spectra of complexes is assigned to π (O) → Cu^{2+} CT transition. The band due to n → π* transition is merged into a broad band in all complexes centered at 29850 cm^{-1} that can be assigned as composite of the remaining n → π* and $\sigma_{(O)} \rightarrow Cu^{2+}$ and other LMCT transitions. The spectra of all complexes exhibit a broad band at 14230–18400 cm^{-1} which consists of at least three overlapping

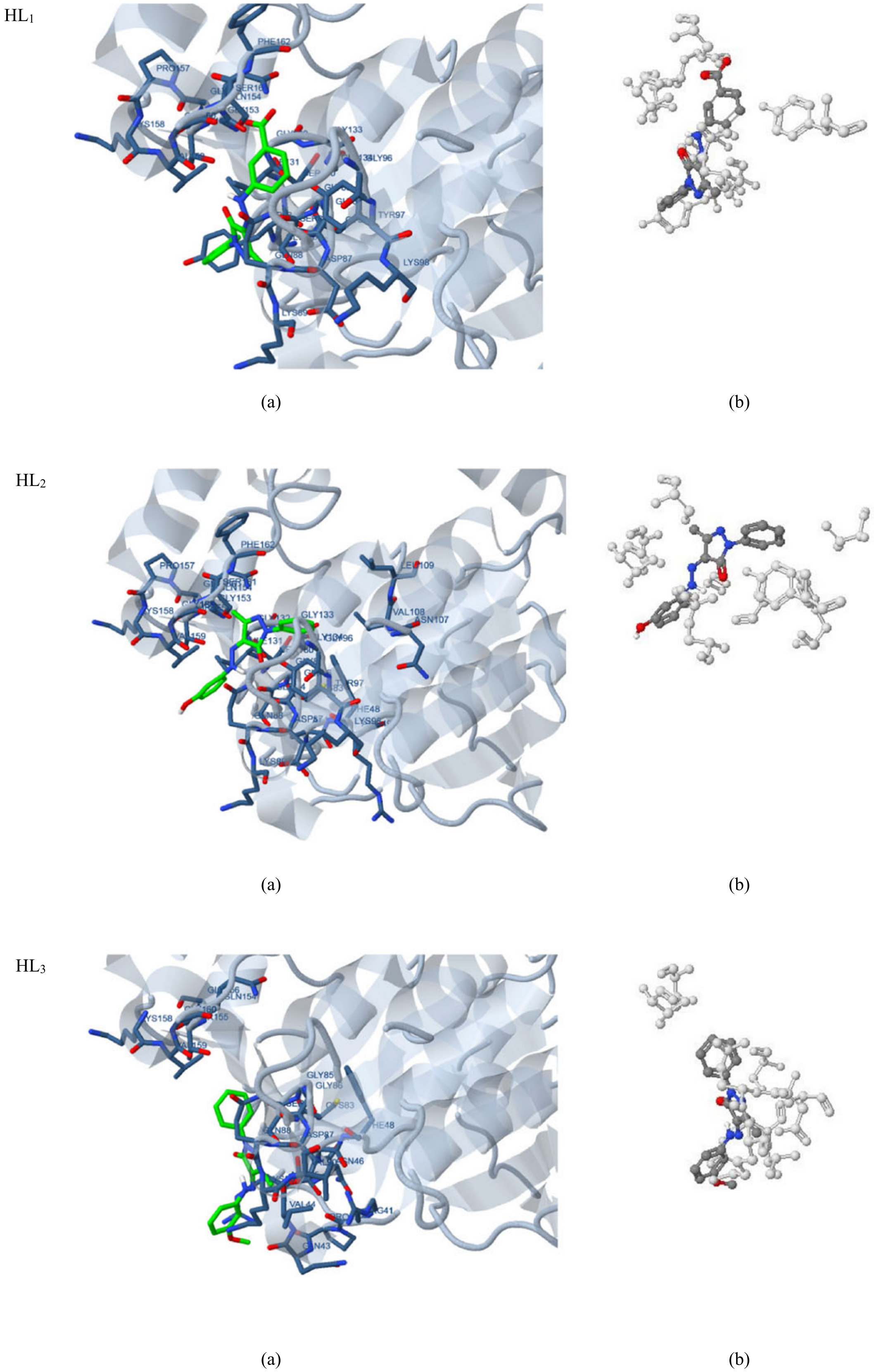

FIGURE 7 Ligands (HL_n) (green in (a) and gray in (b)) in interaction with receptor of crystal structure of *E. coli* (3T88). (For interpretation of the references to color in this figure legend, the reader is referred to the web version of this article)

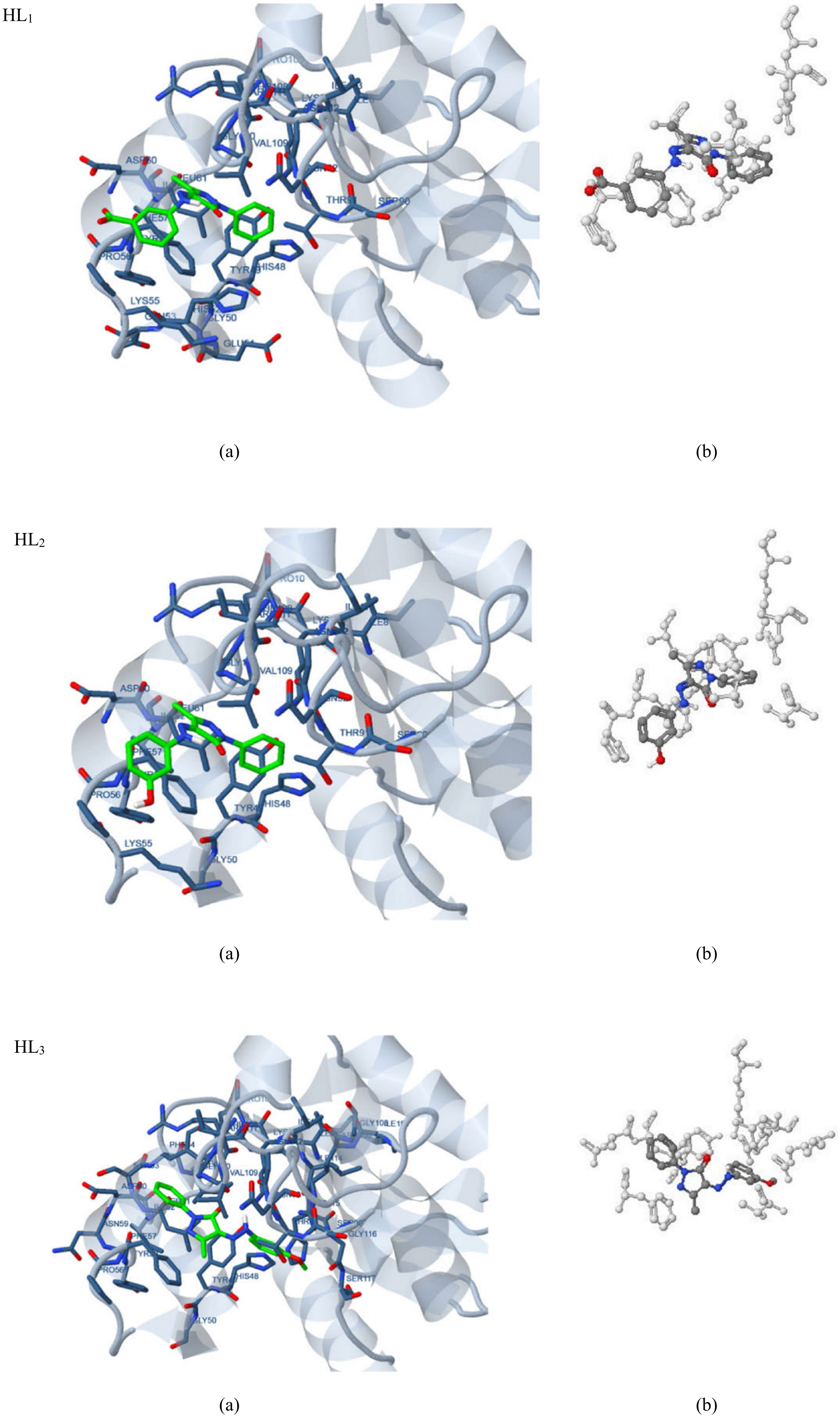

FIGURE 8 Ligands (HL_n) (green in (a) and gray in (b)) in interaction with receptor of crystal structure of *S. aureus* (3Q8U). (For interpretation of the references to color in this figure legend, the reader is referred to the web version of this article)

TABLE 3 Values obtained in docking calculations of ligands (HL_n) with receptors of prostate cancer mutant (2Q7K), breast cancer mutant (3HB5), crystal structure of *E. coli* (3T88) and crystal structure of *S. aureus* (3Q8U)

Code of receptor	Ligand	Est. free energy of binding (kcal/mol)	Est. inhibition constant (K_i) (μM)	vdW+ bond+ desolve energy (kcal/mol)	Electrostatic Energy (kcal/mol)	Total intercooled Energy (kcal/mol)	Interact surface
2Q7K	HL_1	−5.24	144.95	−7.10	+0.06	−7.04	568.175
	HL_2	−6.05	36.65	−7.40	−0.03	−7.43	559.443
	HL_3	−6.38	21.11	−7.88	−0.02	−7.90	574.800
3HB5	HL_1	−7.48	3.31	−8.44	+0.01	−8.43	873.633
	HL_2	−6.72	11.79	−8.48	−0.08	−8.56	823.621
	HL_3	−7.03	7.09	−7.95	+0.02	−7.93	868.268
3T88	HL_1	−6.13	32.38	−7.49	−0.02	−7.51	728.344
	HL_2	−5.27	136.84	−6.14	+0.01	−6.13	715.059
	HL_3	−5.55	85.65	−6.26	−0.08	−6.35	654.252
3Q8U	HL_1	−6.22	27.68	−7.20	+0.06	−7.14	719.779
	HL_2	−5.40	109.32	−6.39	+0.00	−6.38	687.423
	HL_3	−6.02	38.92	−6.83	−0.16	−6.99	805.877

bands. The absorption in this region can be assigned to ligand field transition characteristic of square planar and/or tetrahedrally distorted octahedral copper(II) complexes.[34] The spectral bands are assigned to $^2B_{1g} \rightarrow {}^2Eg$, $^2B_{1g} \rightarrow {}^2B_{2g}$ and $^2B_{1g} \rightarrow {}^2A_{1g}$ transitions.

3.8 | Electronic spin resonance spectral (ESR) studies

ESR spectra studies of paramagnetic Cu(II) complexes gives information about the distribution of the unpaired electrons and hence about the nature of the bonding between the metal ion and its ligands.

3.8.1 | ESR spectra of copper(II) complexes (1–3)

ESR spectra of the present Cu(II) complexes **(1–3)** were recorded at room temperature. The ESR spectra of Cu(II) complexes. The g-values are in the order $g_{\parallel} > g_{\perp} > 2.0023$, indicates the unpaired electron that is corresponding to $d_{x2\text{-}y2}$ orbital as ground state with $3d^9$ configuration. The geometric parameter G, which is a measure of the exchange interaction between copper centers in a polycrystalline compound, is calculated using the equation $G = g_{\parallel}\text{-}2.0023/g_{\perp}\text{-}2.0023$ for axial spectra. If $G > 4$, exchange interaction is negligible and if it is less than 4, considerable exchange interaction is indicated in the solid complex.[35] The calculated G values for these complexes indicate that there are no interactions between the copper centers (Table 4). The value of in-plane σ-bonding parameter α^2 is related to $g_{\parallel}$ and $g_{\perp}$and estimated for each species. The α^2 value of 0.5 indicates complete covalent bonding, while that of 1.0 suggests complete ionic bonding. Since α^2-values obtained lies above 0.5 and below 1.0, which is expected for 100% ionic character of the bonds and become smaller with increasing covalent bonding, it is inferred that the complexes have some covalent character in the ligand environment. The value β^2, which is observed less than unity for the present complexes, also indicates the presence of in-plane π–bonding in the complexes. These findings support that there is significant in-plane σ-bonding and in-plane π-bonding in the complexes[36] the larger the covalency of the bonding.

TABLE 4 ESR spectral assignments of Cu(II) complexes (**1–3**)

Complex[a]	$g_{\parallel}$	$g_{\perp}$	g_{av}	G
(1)	2.392	2.055	2.154	> 4
(2)	2.350	2.100	2.183	> 4
(3)	2.239	2.060	2.120	> 4

[a] Numbers as given in Table 1.

It has been suggested that the smaller value of $A_{\parallel}$ arises from a distortion of a copper site away from planarity.[37] The value of $A_{\parallel} < 140 \times 10^{-4}$ cm^{-1} rules out the possibility of square planar nature (Table S9). The empirical factor f is an index of tetrahedral distortion and its value vary from 105 to 135 for small to extreme distortion in square planar complexes, and that depends on the nature of the coordinated atom.[38] Hence the f values of the complexes are indicating significant distortion from planarity. The value of f can increases markedly on the introduction of tetrahedral distortion to the chromophore. The tetrahedral distortion of a square planar

TABLE 5 ESR spectral assignments of Cu(II) complexes **(4–6)**

Complex[a]	$g_{\parallel}$	$g_{\perp}$	g_{av}	G
(4)	2.245	2.052	2.116	> 4
(5)	2.243	2.060	2.121	> 4
(6)	2.241	2.064	2.123	3.9

[a]Numbers as given in Table 1.

chroimophore with any of the biomimetic (N,O or S) donors reduces $A_{\parallel}$ and increases $g_{\parallel}$, shifting the f values.[39]

3.8.2 | ESR spectra of copper(II) complexes (4–6)

The ESR spectra of all the complexes **(4–6)** (Table 5) are of axial shape with $g_{\parallel} > g_{\perp}$characteristic of complexes with 2B1 ($d_{x2\text{-}y2}$) ground state. In the axial spectra, the g-values are related with exchange interaction coupling constant (G) by the expression G = $g_{\parallel}$-2.0023/$g_{\perp}$-2.0023. According to Hathaway and Tomlinson,[40] if G > 4, the local tetragonal axes are aligned parallel or only slightly misaligned. If G < 4.0, significant exchange coupling is present and the misalignment is appreciable. The calculated G values for these complexes indicate that there are no interactions between the copper interaction between the copper centers (see Table 5). $A_{\parallel}$ for complexes exhibit $g_{\parallel} < 2.3$, suggesting covalent characters of the copper-ligand bonding in the present complexes.

The ESR parameters $g_{\parallel}$, $g_{\perp}$, $A_{\parallel}$ and the energy of the d-d transition were used to evaluate the bonding parameters α^2, β^2 and γ^2, which may be regarded as measures of the covalency of the in-plane σ-bonds, in-plane π-bonds and out-of-plane π-bonds.[12,41] The orbital reduction factors $K_{\parallel} = \alpha^2\beta^2$ and $K_{\perp} = \alpha^2\gamma^2$ were calculated. Significant information about the nature of bonding in the Cu(II) complex can be derived from the relative magnitudes of $K_{\parallel}$ and $K_{\perp}$. In the case of pure σ-bonding, $K_{\parallel} \approx K_{\perp} = 0.77$, whereas $K_{\parallel} < K_{\perp}= 0.77$ implies considerable in-plane π-bonding while for out-of-plane π-bonding $K_{\parallel} > K_{\perp}= 0.77$. For the present complexes, the observed order $K_{\parallel} > K_{\perp}$for complexes **(4)** and **(5)**, while complex **(6)**, $K_{\perp}> K_{\parallel}$ implies a greater contribution from in-plane π-bonding than for out-of-plane. The empirical factor f cm^{-1} is taken as an indication for the stereochemistry of the copper(II) complexes. Addison has suggested that this ratio may be an empirical indication of the tetrahedral distortion of the square planar geometry. The values lower than 135 cm^{-1} are observed for square planar structures and those higher than 150 cm^{-1} for tetrahedrally distorted complexes. The values for the complexes under investigation, Table 5, showed that all complexes associated with tetragonally distorted octahedral ligand field around the copper(II) centers.

The bonding parameters (α^2, β^2 and γ^2) of the complexes have been calculated and summerised (Tables S9 and S10). The bonding parameters α^2, β^2 and γ^2 which may be regarded as measure of the covalency of in-plane σ-bonds, in-plane π-bonds and out-of plane π-bonds, have also been calculated. α^2, β^2 and γ^2 parameters are calculated according to the following equations:[42]

$$\alpha^2 = (A_{\parallel}/0.036) + (g_{\parallel}-2.0023) + 3/7(g_{\perp}-2.0023) + 0.04$$

$$\beta^2 = (g_{\parallel}-2.0023)E/-8\,\lambda\,\alpha^2$$

$$\gamma^2 = (g_{\perp}-2.0023)E/-2\,\lambda\,\alpha^2$$

The λ value is calculated according to Tharmaraj et al.[42] The observed λ value for complexes **(1–6)** (Tables S9 and S10), which is less than that for the free Cu(II) ion (828 cm^{-1}). This reduction in λ from the free ion value is an evidence of covalence in M-L bond.[43] The lower value of λ indicates that there is a considerable mixing of ground and excited state terms.

The ESR data showed that: (i) the value of α^2 of Cu(II) complexes **(4–6)** increases with increasing $g_{av.}$ and $A_{\parallel} \times 10^{-4}$ (Figure S9) and (ii) the value of $g_{\perp}$of Cu(II) complexes **(4–6)** increases with increasing $K^2_{\perp}$as shown in Figure S10.

4 | CONCLUSIONS

HL_n ligands behave as a chelating bidentate monobasic ligands, bonding through NH/CO group and nitrogen atom of the hydrazone group. The electrical conductivities reveal that the complexes are non electrolytes where the anions are bended to the metal ions as indicated by IR.

The data above indicate the possibilities of the significant variation of the structure and, therefore, properties of metal chelate complexes caused by diverse structural modifications of the ligands. Studied in this respect is dominated by problems arise from the influence of strong electron-withdrawing and electron-releasing substituents in the aryl rings of the aromatic and heterocyclic azo compounds, which is essential for defining basicity and ligating abilities of the nitrogen centers in the azo groups. It is expected that the investigation into these problems may be promoted by further extended studies of the series containing relevant azo ligands and gaining deeper insight into the mechanism and preparative application of the azo coupling reactions under the phase transfer catalysis conditions.

ORCID

Sh.M. Morgan http://orcid.org/0000-0002-8921-4894
M.A. Diab http://orcid.org/0000-0002-9042-1356
A.Z. El-Sonbati http://orcid.org/0000-0001-7059-966X

REFERENCES

[1] M. Dakiky, I. Nemcova, *Dyes Pigments* **2000**, *44*, 181.

[2] A. Navarro, F. Sanz, *Dyes Pigments* **1999**, *40*, 131.

[3] J. Tao, G. Mao, L. Daehne, *J. Am. Chem. Soc.* **1999**, *121*, 3475.

[4] S. Vicente, N. Manisso, Z. F. Queiroz, E. A. G. Zagatto, *Talanta* **2002**, *57*, 475.

[5] Sh. M. Morgan, A. Z. El-Sonbati, M. A. El-Mogazy, *Appl. Organometal. Chem.* **2018**, *32*, e4264.

[6] Sh. M Morgan, M. A. Diab, A. Z. El-Sonbati, *Appl. Organometal. Chem.* **2018**, *32*, e4281.

[7] Sh. M. Morgan, M. A. Diab, A. Z. El-Sonbati, *Appl. Organomet. Chem.* **2018**, *32*, e4305.

[8] A. Z. El-Sonbati, M. A. Diab, Sh. M. Morgan, *J. Mol. Liq.* **2017**, *225*, 195.

[9] M. A. Diab, A. Z. El-Sonbati, Sh. M. Morgan, M. A. El-Mogazy, *Appl. Organometal. Chem.* **2018**, *32*, e4378.

[10] H. Park, W. Choi, *J. Photochem. Photobiol. A Chem.* **2003**, *159*, 241.

[11] P. Ball, C. H. Nicholls, *Dyes Pigments* **1982**, *3*, 5.

[12] A. Z. El-Sonbati, M. A. Diab, Sh. M. Morgan, M. Z. Balboula, *Appl. Organometal. Chem.* **2018**, *32*, e4059.

[13] A. Z. El-Sonbati, M. A. Diab, A. A. El-Bindary, Sh. M. Morgan, *Inorg. Chim. Acta* **2015**, *430*, 96.

[14] A. Z. El-Sonbati, M. A. Diab, Sh. M. Morgan, M. A. El-Mogazy, *Appl. Organometal. Chem.* **2018**, e4530.

[15] N. A. El-Ghamaz, M. A. Diab, A. Z. El-Sonbati, O. L. Salem, *Spectrochim. Acta A* **2011**, *83*, 61.

[16] B. S. Furniss, A. S. Hannaford, V. Rogers, P. W. G. Smith, A. R. Tatchell (Eds), *Vogels'Text Book of Practical Organic Chemistry*, fourth ed., ElBS Logman Group Ltd., London **1978**.

[17] A. Z. El-Sonbati, M. A. Diab, Sh. M. Morgan, H. A. Seyam, *J. Mole. Struct.* **2018**, *1154*, 354.

[18] A. Z. El-Sonbati, G. G. Mohamed, A. A. El-Bindary, W. M. I. Hassan, M. A. Diab, Sh. M. Morgan, A. K. Elkholy, *J. Mol. Liq.* **2015**, *212*, 487.

[19] T. A. Halgren, *J. Comput. Chem.* **1998**, *17*, 490.

[20] G. M. Morris, D. S. Goodsell, *J. Comput. Chem.* **1998**, *19*, 1639.

[21] Sh. M. Morgan, A. Z. El-Sonbati, H. R. Eissa, *J. Mol. Liq.* **2017**, *240*, 752.

[22] H. M. Refaat, H. A. El-Badway, Sh. M. Morgan, *J. Mol. Liq.* **2016**, *220*, 802.

[23] G. G. Mohamed, A. A. El-Sherif, M. A. Saad, S. E. A. El-Sawy, Sh. M. Morgan, *J. Mol. Liq.* **2016**, *223*, 1311.

[24] A. Z. El-Sonbati, M. A. Diab, Sh. M. Morgan, A. M. Eldesoky, M. Z. Balboula, *Appl. Organometal. Chem.* **2018**, *32*, e4207.

[25] M. A. Diab, A. Z. El-Sonbati, A. A. El-Bindary, Sh. M. Morgan, *Res. Chem. Intermed.* **2015**, *41*, 9029.

[26] Sh. M. Morgan, N. A. El-Ghamaz, M. A. Diab, *J. Mol. Struct.* **2018**, *1160*, 227.

[27] A. Z. El-Sonbati, M. A. Diab, A. A. El-Bindary, A. M. Eldesoky, Sh. M. Morgan, *Spectrochim. Acta A* **2015**, *135*, 774.

[28] N. A. El-Ghamaz, A. Z. El-Sonbati, Sh. M. Morgan, *J. Mol. Struct.* **2012**, *1027*, 92.

[29] M. I. Abou-Dobara, A. Z. El-Sonbati, Sh. M. Morgan, *World J. Microbiol. Biotechnol.* **2013**, *29*, 119.

[30] A. Z. El-Sonbati, A. A. M. Belal, M. S. El-Gharib, Sh. M. Morgan, *Spectrochim. Acta A* **2012**, *95*, 627.

[31] A. Z. El-Sonbati, M. A. Diab, A. A. M. Belal, Sh. M. Morgan, *Spectrochim. Acta A* **2012**, *99*, 353.

[32] G. J. Karabatoses, B. I. Shapiro, E. M. Vane, J. S. Fleining, J. Ratka, *J. Am. Chem. Soc.* **1931**, *85*, 2784.

[33] A. El-Dissouky, G. B. Mohamad, *Inorganic Theor. Chim. Acta* **1990**, *168*, 241.

[34] A. B. P. Lever, *Inorganic Electronic Spectroscopy*, 2nd ed., Elsevier, New York **1984**.

[35] B. J. Hathaway, D. E. Billing, *Coord. Chem. Rev.* **1970**, *5*, 143.

[36] D. Kivelson, R. Neiman, *J. Chem. Phys.* **1961**, *35*, 149.

[37] P. Peisach, W. E. Blumberg, *Arch. Biochem. Biophys.* **1974**, *165*, 691.

[38] R. Poni, W. C. Bartto, A. Diaz, R. Basosi, *J. Inorg. Biochem.* **2000**, *79*, 333.

[39] U. Sakaguchi, A. W. Addison, *J. Chem. Soc. Dalton Trans.* **1979**, *600*.

[40] B. J. Hathaway, A. A. G. Tomlinson, *Coord. Chem. Rev.* **2004**, *29*, 129.

[41] M. J. Bev, B. J. Hathaway, R. R. Faraday, *J. Chem. Soc. Dalton Trans.* **1972**, *1229*.

[42] P. Tharmaraj, D. Kodimunthiri, C. D. Sheela, C. S. Shanmuga Priya, *J. Serb. Chem. Soc.* **2009**, *74*, 927.

[43] N. Raman, Y. Pitchaikani Raja, A. Kulandaisawy, *Indian Acad. Sci. (Chem. Science)* **2001**, *113*, 183.

SUPPORTING INFORMATION

Additional supporting information may be found online in the Supporting Information section at the end of the article.

How to cite this article: Morgan ShM, Diab MA, El-Sonbati AZ. Supramolecular assembly of hydrogen bonding, ESR studies and theoretical calculations of Cu(II) complexes. *Appl Organometal Chem*. 2018;e4504. https://doi.org/10.1002/aoc.4504